

Lateral diffusion of single poly(ethylene oxide) chains on the surfaces of glassy and molten polymer films

Mears, Matthew; Zhang, Zhenyu J.; Jackson, Ryan C.D.; Si, Yuchen; Bradford, Tigerlily J.B.; Torkelson, John M.; Geoghegan, Mark

DOI:
[10.1063/5.0051351](https://doi.org/10.1063/5.0051351)

License:
Creative Commons: Attribution (CC BY)

Document Version
Publisher's PDF, also known as Version of record

Citation for published version (Harvard):
Mears, M, Zhang, ZJ, Jackson, RCD, Si, Y, Bradford, TJB, Torkelson, JM & Geoghegan, M 2021, 'Lateral diffusion of single poly(ethylene oxide) chains on the surfaces of glassy and molten polymer films', *Journal of Chemical Physics*, vol. 154, no. 16, 164902. <https://doi.org/10.1063/5.0051351>

[Link to publication on Research at Birmingham portal](#)

General rights

Unless a licence is specified above, all rights (including copyright and moral rights) in this document are retained by the authors and/or the copyright holders. The express permission of the copyright holder must be obtained for any use of this material other than for purposes permitted by law.

- Users may freely distribute the URL that is used to identify this publication.
- Users may download and/or print one copy of the publication from the University of Birmingham research portal for the purpose of private study or non-commercial research.
- User may use extracts from the document in line with the concept of 'fair dealing' under the Copyright, Designs and Patents Act 1988 (?)
- Users may not further distribute the material nor use it for the purposes of commercial gain.

Where a licence is displayed above, please note the terms and conditions of the licence govern your use of this document.

When citing, please reference the published version.

Take down policy




While the University of Birmingham exercises care and attention in making items available there are rare occasions when an item has been uploaded in error or has been deemed to be commercially or otherwise sensitive.

If you believe that this is the case for this document, please contact UBIRA@lists.bham.ac.uk providing details and we will remove access to the work immediately and investigate.

Lateral diffusion of single poly(ethylene oxide) chains on the surfaces of glassy and molten polymer films

Cite as: J. Chem. Phys. **154**, 164902 (2021); <https://doi.org/10.1063/5.0051351>

Submitted: 24 March 2021 • Accepted: 07 April 2021 • Published Online: 23 April 2021

 Matthew Mears,  Zhenyu J. Zhang,  Ryan C. D. Jackson, et al.



View Online



Export Citation



CrossMark

ARTICLES YOU MAY BE INTERESTED IN

[Effect of surface properties and polymer chain length on polymer adsorption in solution](#)
The Journal of Chemical Physics **155**, 034701 (2021); <https://doi.org/10.1063/5.0052121>

[Machine learning meets chemical physics](#)
The Journal of Chemical Physics **154**, 160401 (2021); <https://doi.org/10.1063/5.0051418>

[Ordering, phase behavior, and correlations of semiflexible polymers in confinement](#)
The Journal of Chemical Physics **154**, 090901 (2021); <https://doi.org/10.1063/5.0038052>

The Journal
of Chemical Physics

SPECIAL TOPIC: Low-Dimensional
Materials for Quantum Information Science

Submit Today!

Lateral diffusion of single poly(ethylene oxide) chains on the surfaces of glassy and molten polymer films

Cite as: J. Chem. Phys. 154, 164902 (2021); doi: 10.1063/5.0051351

Submitted: 24 March 2021 • Accepted: 7 April 2021 •

Published Online: 23 April 2021










View Online



Export Citation



CrossMark

Matthew Mears,¹  Zhenyu J. Zhang,^{1,a)}  Ryan C. D. Jackson,^{1,b)}  Yuchen Si,^{1,c)}  Tigerlily J. B. Bradford,^{1,d)} 
John M. Torkelson,²  and Mark Geoghegan^{1,e)} 

AFFILIATIONS

¹Department of Physics and Astronomy, University of Sheffield, Sheffield S3 7RH, United Kingdom

²Department of Chemical and Biological Engineering and Department of Materials Science and Engineering, Northwestern University, Evanston, Illinois 60208, USA

^{a)}Present address: School of Chemical Engineering, University of Birmingham, Birmingham B15 2TT, UK.

^{b)}Present address: Department of Chemistry, Durham University, South Road, Durham DH1 3LE, UK.

^{c)}Present address: School of Physics and Astronomy, University of Edinburgh, Edinburgh EH9 3FD, UK.

^{d)}Present address: Department of Chemistry, Imperial College London, White City Campus, London W12 7TA, UK.

^{e)}Present address: School of Engineering, Newcastle University, Merz Court, Newcastle-upon-Tyne NE1 7RU, UK.

Author to whom correspondence should be addressed: mark.geoghegan@newcastle.ac.uk

ABSTRACT

Fluorescence correlation spectroscopy was used to show that the temperature-dependent diffusion coefficient of poly(ethylene oxide) (PEO) adsorbed on polystyrene and different poly(alkyl methacrylate) (PAMA) films in aqueous solution exhibited a maximum close to (but below) the surface glass transition temperature, T_{gs} , of the film. This elevated diffusion was observed over a small range of temperatures below T_{gs} for these surfaces, and at other temperatures, the diffusion was similar to that on silicon, although the diffusion coefficient for PEO on polystyrene at temperatures above T_{gs} did not completely decrease to that on silicon, in contrast to the PAMA surfaces. It is concluded that the enhanced surface mobility of the films near the surface glass transition temperature induces conformational changes in the adsorbed PEO. The origin of this narrow and dramatic increase in diffusion coefficient is not clear, but it is proposed that it is caused by a coupling of a dominant capillary mode in the liquid surface layer with the polymer. Friction force microscopy experiments also demonstrate an unexpected increase in friction at the same temperature as the increase in diffusion coefficient.

© 2021 Author(s). All article content, except where otherwise noted, is licensed under a Creative Commons Attribution (CC BY) license (<http://creativecommons.org/licenses/by/4.0/>). <https://doi.org/10.1063/5.0051351>

I. INTRODUCTION

Molecular theory underpinning the physics of the glass transition in polymers is still lacking, but the dramatic effect of confinement on the glass transition has been known for some time to play a key role.^{1–4} The original experiments on thin films of polystyrene⁵ and, shortly after, poly(methyl methacrylate) (PMMA)⁶ demonstrated that there was a significant reduction in the glass transition temperature (T_g) with film thickness, but could provide only an empirical description of their behavior. Despite the difficulties that traditional semi-empirical free volume theories have

experienced, the concept of free volume as a means to explain the glass transition of confined polymer films has remained remarkably robust.^{3,4,7,8}

An important early question was related to whether confinement or the free surface of the film was responsible for the depressed glass transition. Early experiments on dewetting were explained by arguing that thinner films were less dense than in the bulk, and consequently, the effective glass transition temperature was reduced.⁹ These arguments contradicted a popular idea that chain conformations were unperturbed by a surface,^{10,11} but it has subsequently been accepted that polymers near the surface of a film do not have

the same conformation as those deeper into the film.^{12–14} Later, experiments were able to identify that the glass transition increased with distance from the surface of the film,¹⁵ although this effect was strongly dependent upon the chemical nature of the polymer beneath the surface layer.¹⁶ It has since been argued that a discrete liquid surface layer occurs below the bulk T_g for both entangled and unentangled films.¹⁷

On the one hand, the surface presents itself as an interface to a semi-infinite reservoir of free volume,¹⁸ which aids relaxation of the chains, but on the other hand, the surface perturbs the film itself, increasing the segmental mobility in its vicinity.¹⁹ The surface therefore plays a profound role in the depressed glass transition of polymer films. The glass transition in a fluid environment is less understood, although work on polystyrene films and nanoparticles suggests that an aqueous interface with the film does not noticeably change the depression in the glass transition temperature.²⁰

The lateral diffusion of polymers on surfaces is an ideal means of testing for changes in the behavior of that surface because it strongly depends on the nature of the adsorption.²¹ A polymer that is fully adsorbed in a “pancake” configuration²² on the surface is constrained and exhibits less movement than one that has fewer contact points on the surface.²³ The diffusion of poly(ethylene oxide) (PEO) on surfaces is a function of other parameters such as the concentration of adsorbed polymer^{24–27} or the presence of topographic constraints.^{28,29} All of these experiments concern the diffusion at the solid–liquid interface. Little is known of how a polymer diffuses at the aqueous interface with a molten polymer film, which is subject to capillary waves, which themselves are influenced by the surface melting associated with the glass transition.³⁰

In this work, single poly(ethylene oxide) (PEO) chains are allowed to diffuse in an aqueous environment on polymer surfaces as a function of temperature. The surfaces comprised polystyrene and different poly(alkyl methacrylate) (PAMA) homopolymer and blend films. It is proposed that there is a coupling of the polymer to the surface of the film ~ 10 K below the surface glass transition, which causes a large increase in the surface diffusion of the PEO over a narrow temperature range. A similar effect is observed using friction force microscopy (FFM).

II. EXPERIMENTAL

A. Polymer films

Silicon substrates (Prolog Semicor, Ukraine) were cleaved into ~ 1 cm² sections, sonicated in chloroform and then toluene for ~ 20 min in each, and cleaned for ~ 15 min in an oxygen plasma. The cleaned substrates were then immediately coated with the relevant polymer by spin coating. Solutions of 5% w/v poly(alkyl methacrylate) or polystyrene in toluene were used, and spin speeds ranging from 2000 to 4000 rpm allowed the control of the resulting film thickness to be between ~ 250 and 350 nm.

The polymers used for the films were PMMA (mass averaged molar mass, $M = 120$ kDa, and dispersity, $\mathcal{D} = 2.0$), PEMA ($M = 250$ kDa and $\mathcal{D} = 2.3$), PPMA ($M = 150$ kDa and $\mathcal{D} = 2.4$), PBMA ($M = 337$ kDa and $\mathcal{D} = 2.1$), and polystyrene ($M = 222$ kDa

and $\mathcal{D} = 1.02$). All polymers were purchased from Sigma-Aldrich and used as received.

The resulting films were incubated at 353 K for a minimum of 8 h to allow any residual solvent to leave the film. Homopolymer films were heated to ~ 30 K above the surface glass transition temperature, T_{gs} , and held at this temperature for at least 1 h in order to allow the polymer chains to relax toward an equilibrium state before cooling at a constant rate of 2 K min⁻¹ to ~ 30 K below T_{gs} before performing fluorescence correlation spectroscopy (FCS) experiments. Experiments were also performed using blends of PBMA and PMMA, which were heated to 393 K for at least 1 h to allow both polymer components of the film to relax and then cooled at 2 K min⁻¹ to ~ 280 K. Low temperature ellipsometry measurements were performed with the aid of a liquid nitrogen flow-cooled chamber, but FCS measurements were limited to ~ 278 K to avoid condensation, precluding measurements using PBMA homopolymer films.

B. Ellipsometry measurements

The thickness of the films was determined using an M-2000 spectroscopic ellipsometer (J. A. Woollam Co., Inc.). The film temperatures were controlled using a Linkam heating stage (Linkam Scientific Instruments Ltd., Surrey, UK) with a TMS94 heat controller and LNP-1 nitrogen flow control. The Linkam stage was calibrated using the boiling points of various solvents. An ellipsometry-specific sealed chamber (Linkam Scientific Instruments Ltd.) with a nitrogen gas flow was used to minimize atmospheric effects for thickness measurements.

A Cauchy model was developed and used within the native software to fit the data and extract the thickness. The resulting temperature–thickness curves were subsequently analyzed using the pro Fit v6.1.16 (QuantumSoft, Switzerland) software package to determine the glass transition temperatures (Fig. S1).

C. Diffusion measurements

FCS measurements were performed using an LSM510 AxioVert inverted confocal microscope with a ConfoCor2 FCS module (Carl Zeiss, Germany). Alignment and calibration of the optics were performed using 10 μ M fluorescein isothiocyanate in water, and diffusion measurements were performed with fluorescein-labeled PEO ($M = 20$ kDa and $\mathcal{D} = 1.2$, purchased from Scientific Polymer Products, Inc, Ontario, USA, and used as received). Fluorescein was excited using the 488 nm line of an argon laser, and fluorescence emission was collected through a 510–560 nm bandpass filter and recorded with an avalanche photodiode. The film temperatures were controlled using a Linkam heating stage (Linkam Scientific Instruments Ltd.) with a TMS94 heat controller and LNP-1 nitrogen flow control. A custom-built mount was used to invert and secure the heating stage onto the microscope platform for FCS measurements. A ~ 5 nM solution of fluorescein isothiocyanate-labeled PEO was prepared in water, and a small volume (< 10 μ l) was placed onto the film before mounting onto the microscope stage. The droplet was confined between the polymer film and microscope objective lens, so evaporation was kept to a minimum. Little change in concentration was observed during the experiments. Experiments were performed on heating the samples, but cooling

the samples from an elevated temperature yielded identical results (Fig. S3).

Accurate positioning of the confocal volume onto the surface of the film was critical in preventing the introduction of artifacts into the correlation curves, particularly because silicon substrates can act as a mirror and amplify noise as well as the signal. The confocal volume was first coarsely focused close to the surface using the on-screen image, after which z -scanning was performed in 100 nm steps from the bulk solution toward the coated surface. The position of the surface was determined by the peak signal-to-noise ratio from the automated z -positioning of the ConfoCor2 system. The surface diffusion signal was always significantly larger than that of bulk diffusion and so was easy to identify. Typically, the number, N , of labeled PEO on the surface over all temperatures was $3 < N < 7$. There was little variation in N with temperature. In order to eliminate any effect due to variations in temperature across the surface, the data were all obtained at the same point on the film at each temperature. After allowing 15 min equilibration time at each temperature, the data were taken over a period of 1 h. The long measurement times over a complete temperature scan did not cause any problems, as can be concluded from the heating and cooling scans (Fig. S3).

The autocorrelation data were extracted from the native Zeiss software and fitted using the pro Fit software package with the autocorrelation function including both three- and two-dimensional components.³¹ The autocorrelation function is given by

$$G(\tau) = 1 + \frac{1}{N} \left(\frac{(1-f)}{\left(1 + \frac{\tau}{\tau_{3D}}\right) \sqrt{1 + \frac{\tau}{\tau_{3D}\Gamma^2}}} + \frac{f}{1 + \frac{\tau}{\tau_{2D}}} \right) \times \left(1 + \left(\frac{P_t}{1 - P_t} \right) \exp\left(\frac{-\tau}{\tau_t}\right) \right), \quad (1)$$

where f is the fraction of molecules adsorbed onto film, τ_{3D} is the diffusion time of free molecules, Γ is the structure parameter of the confocal volume ($4 < \Gamma < 11$, dependent upon the width of the confocal volume) and was fixed from control measurements of fluorescein dye, and τ_{2D} is the diffusion time of adsorbed molecules. The excitation of electrons into the triplet state is quantified by the triplet lifetime τ_t and the population of the triplet state, P_t .^{32,33} This model assumes isotropic two-dimensional diffusion on a homogeneous surface and reduces to the standard bulk autocorrelation function when the confocal volume is moved into the solution (and hence $f = 0$).

The autocorrelation data were fitted with the above model for times greater than $2 \mu\text{s}$ to avoid distortions introduced from afterpulsing in the avalanche detector. The data were analyzed by Levenberg-Marquardt nonlinear least-squares fitting using the pro Fit software package (6.2.9). Surface diffusion coefficients were relatively easy to obtain because the bulk diffusion time was usually well separated from that due to surface diffusion and did not contribute significantly. There was also no observable contribution of free dye in these experiments. Fluorescein has a large diffusion coefficient ($>400 \mu\text{m}^2 \text{s}^{-1}$) in water.³⁴⁻³⁶ N dictated the amplitude of the autocorrelation function and did not interfere with the fitting of τ_{2D} . The only other fitting parameter was f , which controls the relative contributions of surface and bulk diffusion and was thus easily extracted. Under the conditions of the experiment, f was close to unity. Some

diffusion times were measured repeatedly in order to obtain the error in the diffusion coefficients. This error was estimated to be $\pm 5\%$ and was independent of temperature.

D. Friction force microscopy

A Digital Instruments Dimension 3100 atomic force microscope (AFM) with Nanoscope IV controller (Veeco, Cambridge, UK) was operated in contact mode with a liquid cell/tip holder. Silicon nitride probes (SNL, Bruker, California, USA) with nominal spring constant 0.12 Nm^{-1} and tip radius 2 nm were used. FFM measurements were performed at a scan rate of 2.03 Hz with 256 data points per line and with a scan area of $1 \times 1 \mu\text{m}^2$. Each cantilever was calibrated by a Digital Instruments PicoForce module and its associated software based on the method of Hutter and Bechhoefer,³⁷ confirming the nominal value supplied. The optical lever sensitivity of each modified cantilever was calibrated in de-ionized water at room temperature before each set of experiments. The friction force was acquired by converting the lateral signal collected by the photodetector from voltage to newton using the wedge method,^{38,39} where the cantilever is scanned across a calibration grating (TGF11, MikroMasch, Tallinn, Estonia) and the frictional signal is measured as a function of applied load.

III. RESULTS

A. Glass transition temperatures

The glass transition temperatures of films of these polymers were measured by determining the change in expansivity by ellipsometry.⁵ The film temperatures were controlled using a Linkam heating stage under nitrogen flow. The film is taken to comprise a solid and liquid layer with a total thickness dependent upon T_{gs} and T_{gb} , the surface and bulk glass transition temperatures, and their corresponding liquid and solid (glass) expansion coefficients. The film thickness can be fitted using a simple model.⁴⁰ These glass transition temperatures obtained from the ellipsometry data are tabulated in Table I, which includes d_{gs} , the film thickness at $T = T_{gs}$.

For the measurement of surface diffusion, fluorescein isothiocyanate end-labeled PEO ($M = 20 \text{ kDa}$) was allowed to adsorb from a dilute solution in water onto the polymer film with a clean uncoated silicon wafer used as a control. Diffusion coefficients of PEO were measured using fluorescence correlation spectroscopy (FCS).³² Sample FCS data (autocorrelation functions) and fits are shown in Fig. 1.

TABLE I. Glass transition temperatures as measured using ellipsometry.

B. Polymer	T_{gs} (K)	T_{gb} (K)	d_{gs} (nm)
PMMA	373 ± 7	403 ± 8	252
PEMA	341 ± 5	367 ± 6	282
PPMA	308 ± 3	325 ± 4	352
PBMA	269 ± 3	331 ± 8	279
Polystyrene	356 ± 4	387 ± 5	232

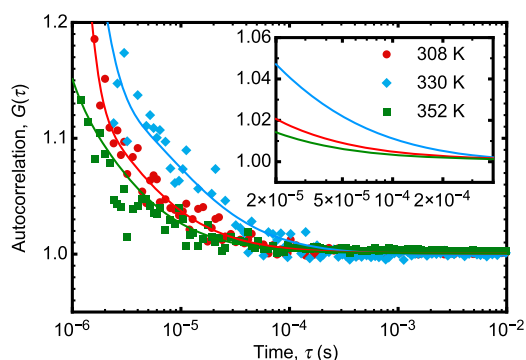


FIG. 1. FCS autocorrelation function data and fits for PEO on PEMA films at three different temperatures. The triplet states and bulk diffusion dominate the data at early times, and the shorter (surface) diffusion time of the data at 330 K is significant from $\tau \approx 10^{-4}$ s. The fits to the data are shown in the inset, which covers the period where surface diffusion dominates. Here, the autocorrelation function has the steepest decay for the sample measured at 330 K, indicating the shortest diffusion time, and thus the largest diffusion coefficient.

The measured diffusion coefficients are plotted in Fig. 2(a). The diffusion of PEO on the uncoated silicon wafer follows a simple linear dependence with temperature, as would be expected for the Stokes–Einstein behavior. The diffusion of PEO on different

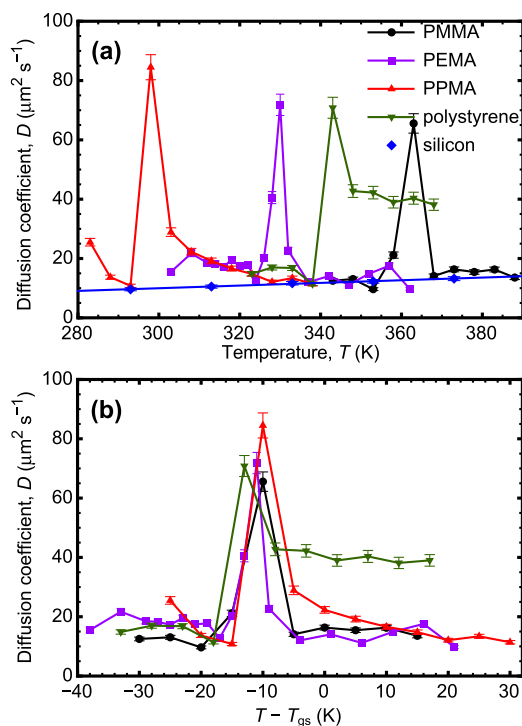


FIG. 2. (a) Diffusion profiles of PEO adsorbed onto polymer films for temperatures around their glass transitions. The diffusion coefficients for PEO adsorbed onto bare silicon are also shown. The diffusion coefficients are guides to the eye, except for the results for PEO on silicon, for which the solid line is a linear fit to temperature. (b) The same diffusion profiles as in (a), but with the temperature scale relative to the surface glass transition temperature T_{gs} , as determined using ellipsometry.

poly(alkyl methacrylate) films also exhibits this behavior, except for temperatures given by $T_{gs} - T \approx 10$ K [Fig. 2(b)], where there is a notable increase in the diffusion coefficient. In addition, PEO was allowed to diffuse on films of blends of PMMA and PBMA, which, being immiscible, exhibit two glass transitions. PBMA and PMMA have a reported interaction parameter of $\chi = 0.062$ at $T = 413$ K based on a lattice size of 0.72 nm⁴¹ and are expected to exhibit an upper critical solution temperature, as is the case for PEMA and PMMA.⁴² Diffusion coefficients for PEO on films of blends of PMMA and PBMA are shown in Fig. 3. The maximum diffusion coefficients are similar to those in the bulk solution for PEO of similar molar mass.^{22,26,28}

The blend data reveal two peaks in the diffusion coefficient: one corresponding to the glass transition temperature of the PBMA-rich phase and the other corresponding to that of the PMMA-rich phase. In both cases, the peaks are located ~ 10 K below the corresponding expansivity change measured using ellipsometry (Fig. S1b). Only one PEO surface diffusion coefficient was obtained from fitting the blend data at each temperature.

On polystyrene, the PEO also exhibited a separate peak in surface diffusion. In contrast to its behavior on poly(alkyl methacrylate) surfaces, at temperatures greater than those corresponding to the peak in the diffusion coefficient, the PEO diffusion on polystyrene did not return to the same behavior exhibited at lower temperatures (Fig. 2). It has been well documented that

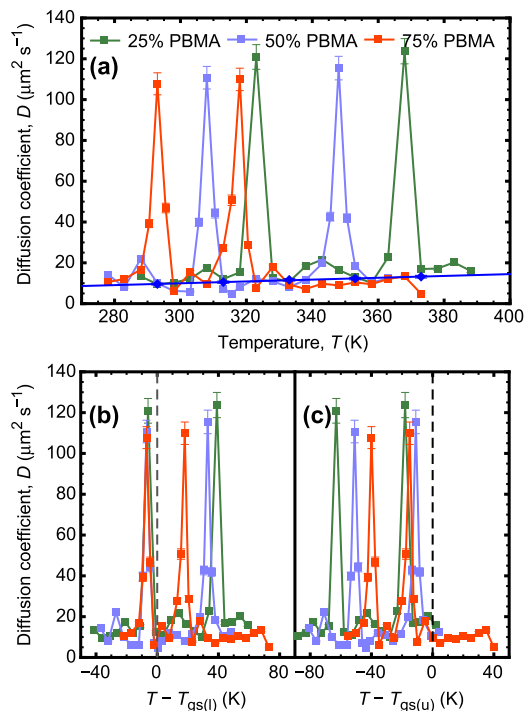


FIG. 3. (a) The diffusion of PEO as a function of temperature on blends of PBMA and PMMA revealed two peaks in the diffusion coefficient for each blend, indicating two glass transitions. The temperatures are plotted relative to the temperatures of the lower (b), $T_{gs(l)}$, and upper (c), $T_{gs(u)}$, transitions, which are indicated by the broken vertical lines.

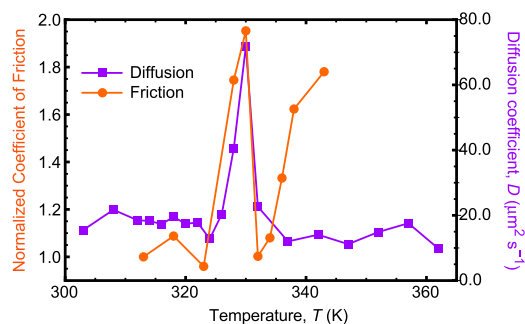


FIG. 4. FFM data reveal a peak in the coefficient of friction of a silicon nitride AFM tip on a PEMA surface. The friction data are normalized to the result at 313 K.

PEO-poly(alkyl methacrylate) blends are at least partially miscible^{43–46} in which case adsorbed PEO has a similar attractive interaction with the poly(alkyl methacrylate) film both above and below T_{gs} . The same does not apply to PEO and polystyrene, which are highly immiscible.⁴⁷

In order to directly interrogate the surface of the polymer films, friction force microscopy (FFM)⁴⁸ was performed on a PEMA film under water as a function of temperature. In Fig. 4, the FFM data are shown for a PEMA film with the diffusion coefficient of PEO on the same surface also shown for comparison. The friction coefficient of PEMA increases with temperature above its glass transition, as would be expected for a film close to its melting point. However, again at $T_{gs}-T \approx 10$ K, a narrow peak can be observed. The increase in friction coefficient near, but below, the glass transition temperature of PEMA is unexpected, but more comprehensive studies have revealed the existence of an increase in frictional behavior close to the glass transition in polystyrene films.⁴⁹ The FFM setup used in this work can only be operated over a limited temperature range, so these experiments were restricted to PEMA films.

IV. DISCUSSION

The large increase in diffusion coefficient indicates a PEO conformational transition at $T = T_{gs}-10$ K. PEO fully adsorbed onto a substrate (pancake structure) has a diffusion coefficient an order of magnitude smaller than that when it takes up a conformation comprising loops and trains,²³ so it can be concluded that the surface of the polymer film triggers a conformational change in the PEO. However, it is not likely that PEO has a flat (pancake) structure on these films; previous measurements have indicated that when it has a pancake structure (20 kDa), PEO diffuses with a coefficient close to $0.1 \mu\text{m}^2/\text{s}$,²² which is smaller than the values measured here. PEO is also reticent to adsorb to PMMA, silica, or polystyrene.⁵⁰ This PEO takes up a pancake structure that has been questioned for hydrophobic surfaces,⁵¹ but force spectroscopy has revealed that adsorption as a pancake structure does occur on some surfaces.²³ Bulk measurements of PEO diffusion have a diffusion coefficient similar to the maximum surface diffusion values reported here,^{22,26,28} and so it may be argued that the conformational transition just below the glass transition amounts to desorption. Nevertheless, the relative

contributions of adsorption and desorption are important in some diffusion mechanisms.^{52,53}

Both poly(alkyl methacrylate) films and the native oxide layer of silicon surfaces offer hydrogen bonding sites with which the PEO can interact. In order to test the effect of nonpolar surfaces on the diffusion, polystyrene films were used. As can be seen in Fig. 2(a), there is again a peak in the diffusion coefficient at $T \approx T_{gs}-10$ K. However, at greater temperatures, the diffusion coefficient does not return to values of the silicon or the poly(alkyl methacrylate) films but remains at a large value, albeit below the maximum. It is known, however, that PEO undergoes a conformational transition at temperatures greater than its θ -temperature⁵⁴ and that its adsorption to polystyrene is affected.⁵⁵ The related possibility that the more polar poly(alkyl methacrylate) films might absorb some water deserves some consideration. However, the finding that PEO exhibits a peak in its diffusion coefficient on both polystyrene and poly(alkyl methacrylate) films at ~ 10 K below the surface glass transition shows that the swelling of these films by water is not a significant effect. Earlier neutron reflectometry experiments have also shown limited water swelling of glassy PMMA and rubbery PBMA films.⁵⁶

A recent report has shown that tobacco mosaic virus (TMV) diffuses on the surface of a glassy film of N,N' -bis(3-methylphenyl)- N,N' -diphenylbenzidine independent of film thickness, despite the observed film thickness dependence of the glass transition temperature.⁵⁷ The conclusion from this work was that, near the glass transition, there was a discrete layer of greater segmental mobility, the properties of which were independent of the underlying film. This conclusion is consistent with the present results. Nevertheless, the limited temperature dependence of the TMV surface diffusion experiments does not allow a direct comparison. Furthermore, the TMV is large and asymmetric⁵⁸ and perhaps not an ideal comparator.

As can be seen in Fig. 4, there is a peak in the friction coefficient at a similar temperature to that in the diffusion coefficient (also shown). A proxy for temperature is that of time, and by changing the scanning rate, it has been shown elsewhere that the glass transition has an effect on the time-temperature superposition coefficient at the glass transition for polystyrene.⁴⁹ Other experiments performed using AFM to determine mechanical properties of nanoparticle-embedded polystyrene also provide evidence for a shift in the behavior in the vicinity of the glass transition, where evidence of surface stiffening was found.⁵⁹

Ultimately, a sharp AFM tip interacting with the polymer surface may be of comparable size to 20 kDa PEO and it is possible that the size of the object, which perturbs the film, is relevant. As has been pointed out,³⁰ a thin layer has associated capillary waves that have a dominant wavelength of $\lambda \approx 2\pi h$, where h is the film thickness. Longer wavelengths will be impeded by the thickness of the layer, and shorter ones will be thermodynamically suppressed because they create too much interface. The tantalizing suggestion that a dominant mode couples to the adsorbed polymer can only be tested by a comprehensive study covering a large range of molar masses.

V. CONCLUSIONS

To summarize, the data have been presented to show that the nature of the surface of the film has a profound effect on the

diffusion of polymers adsorbed on that film. At temperatures some 10 K below the surface glass transition, an anomalous peak in the diffusion coefficient is observed, the origin of which is unclear, but it may be speculated that the adsorbed PEO is interacting with a nanoscale surface layer. This behavior is observed for PEO adsorbed on polystyrene films and three poly(alkyl methacrylate) films, as well as blends of PBMA and PMMA, and may therefore be considered to be a general phenomenon.

SUPPLEMENTARY MATERIAL

See the [supplementary material](#) for ellipsometry thickness results, FCS hysteresis data and results for the diffusion of dextran on PEMA, which also show a diffusion maximum, water contact angle analysis, and scanning force and optical microscopy images of blend films.

ACKNOWLEDGMENTS

The EPSRC is acknowledged for providing financial support through a doctoral training award for MM and through Grant No. EP/I012060/1 for Z.J.Z. David Spiller at the University of Manchester is acknowledged for help with the FCS experiments of dextran presented in the [supplementary material](#).

DATA AVAILABILITY

The data that support the findings of this study are available from the corresponding author upon reasonable request. Raw FCS data are available on the University of Sheffield Online Research Data archive at <https://doi.org/10.15131/shef.data.14390495> (Ref. 60).

REFERENCES

- 1 M. Alcoutlabi and G. B. McKenna, *J. Phys.: Condens. Matter* **17**, R461 (2005).
- 2 M. D. Ediger and J. A. Forrest, *Macromolecules* **47**, 471 (2014).
- 3 S. Napolitano, E. Glynos, and N. B. Tito, *Rep. Prog. Phys.* **80**, 036602 (2017).
- 4 K. S. Schweizer and D. S. Simmons, *J. Chem. Phys.* **151**, 240901 (2019).
- 5 J. L. Keddie, R. A. L. Jones, and R. A. Cory, *Europhys. Lett.* **27**, 59 (1994).
- 6 J. L. Keddie, R. A. L. Jones, and R. A. Cory, *Faraday Discuss.* **98**, 219 (1994).
- 7 A. Debot, R. P. White, J. E. G. Lipson, and S. Napolitano, *ACS Macro Lett.* **8**, 41 (2019).
- 8 R. P. White and J. E. G. Lipson, *Macromolecules* **49**, 3987 (2016).
- 9 G. Reiter, *Europhys. Lett.* **23**, 579 (1993).
- 10 R. L. Jones, S. K. Kumar, D. L. Ho, R. M. Briber, and T. P. Russell, *Macromolecules* **34**, 559 (2001).
- 11 A. Silberberg, *J. Colloid Interface Sci.* **90**, 86 (1982).
- 12 A. Brület, F. Boué, A. Menelle, and J. P. Cotton, *Macromolecules* **33**, 997 (2000).
- 13 M. Geoghegan and G. Krausch, *Prog. Polym. Sci.* **28**, 261 (2003).
- 14 N. Rehse, C. Wang, M. Hund, M. Geoghegan, R. Magerle, and G. Krausch, *Eur. Phys. J. E* **4**, 69 (2001).
- 15 C. J. Ellison and J. M. Torkelson, *Nat. Mater.* **2**, 695 (2003).
- 16 C. B. Roth, K. L. McNerny, W. F. Jager, and J. M. Torkelson, *Macromolecules* **40**, 2568 (2007).
- 17 Z. Yang, A. Clough, C.-H. Lam, and O. K. C. Tsui, *Macromolecules* **44**, 8294 (2011).
- 18 V. M. Boucher, D. Cangialosi, H. Yin, A. Schönhal, A. Alegría, and J. Colmenero, *Soft Matter* **8**, 5119 (2012).
- 19 J. A. Forrest and K. Dalnoki-Veress, *ACS Macro Lett.* **3**, 310 (2014).
- 20 C. Zhang, Y. Guo, and R. D. Priestley, *Macromolecules* **44**, 4001 (2011).
- 21 M. Mears, Z. Zhang, R. Tarmey, and M. Geoghegan, *Macromol. Rapid Commun.* **32**, 1411 (2011).
- 22 S. A. Sukhishvili, Y. Chen, J. D. Müller, E. Gratton, K. S. Schweizer, and S. Granick, *Nature* **406**, 146 (2000).
- 23 P. Burgos, Z. Zhang, R. Golestanian, G. J. Leggett, and M. Geoghegan, *ACS Nano* **3**, 3235 (2009).
- 24 G. T. Morrin and D. K. Schwartz, *Macromolecules* **51**, 1207 (2018).
- 25 D. Mukherji and M. H. Müser, *Phys. Rev. E* **74**, 010601(R) (2006).
- 26 Z. J. Zhang, S. Edmondson, M. Mears, J. Madsen, S. P. Armes, G. J. Leggett, and M. Geoghegan, *Macromolecules* **51**, 6312 (2018).
- 27 J. Zhao and S. Granick, *J. Am. Chem. Soc.* **126**, 6242 (2004).
- 28 C. G. Clarkson, A. Johnson, G. J. Leggett, and M. Geoghegan, *Nanoscale* **11**, 6052 (2019).
- 29 D. Wang, C. He, M. P. Stoykovich, and D. K. Schwartz, *ACS Nano* **9**, 1656 (2015).
- 30 S. Herminghaus, R. Seemann, and K. Landfester, *Phys. Rev. Lett.* **93**, 017801 (2004).
- 31 E. L. Elson and D. Magde, *Biopolymers* **13**, 1 (1974).
- 32 E. Haustein and P. Schuille, *Annu. Rev. Biophys. Biomol. Struct.* **36**, 151 (2007).
- 33 J. Widengren, U. Mets, and R. Rigler, *J. Phys. Chem.* **99**, 13368 (1995).
- 34 C. T. Culbertson, S. C. Jacobson, and J. M. Ramsey, *Talanta* **56**, 365 (2002).
- 35 P. H. Paul, M. G. Garguilo, and D. J. Rakestraw, *Anal. Chem.* **70**, 2459 (1998).
- 36 Z. Petrásek and P. Schuille, *Biophys. J.* **94**, 1437 (2008).
- 37 J. L. Hutter and J. Bechhoefer, *Rev. Sci. Instrum.* **64**, 1868 (1993).
- 38 D. F. Ogletree, R. W. Carpick, and M. Salmeron, *Rev. Sci. Instrum.* **67**, 3298 (1996).
- 39 M. Varenberg, I. Etsion, and G. Halperin, *Rev. Sci. Instrum.* **74**, 3362 (2003).
- 40 J. E. G. Lipson and S. T. Milner, *Macromolecules* **43**, 9874 (2010).
- 41 J. Scherble, B. Stark, B. Stühn, J. Kressler, H. Budde, S. Höring, D. W. Schubert, P. Simon, and M. Stamm, *Macromolecules* **32**, 1859 (1999).
- 42 J. A. Schroeder, F. E. Karasz, and W. J. MacKnight, *Polymer* **26**, 1795 (1985).
- 43 R. H. Colby, *Polymer* **30**, 1275 (1989).
- 44 M. Dionísio, A. C. Fernandes, J. F. Mano, N. T. Correia, and R. C. Sousa, *Macromolecules* **33**, 1002 (2000).
- 45 E. E. Shafee and W. Ueda, *Eur. Polym. J.* **38**, 1327 (2002).
- 46 J. A. Zawada, C. M. Ylitalo, G. G. Fuller, R. H. Colby, and T. E. Long, *Macromolecules* **25**, 2896 (1992).
- 47 E. Yilmaz, O. Yilmaz, and H. Caner, *Eur. Polym. J.* **32**, 927 (1996).
- 48 R. W. Carpick and M. Salmeron, *Chem. Rev.* **97**, 1163 (1997).
- 49 T. Kajiyama, K. Tanaka, N. Satomi, and A. Takahara, *Macromolecules* **31**, 5150 (1998).
- 50 C.-y. Chen, M. A. Even, J. Wang, and Z. Chen, *Macromolecules* **35**, 9130 (2002).
- 51 M. J. Skaug, J. N. Mabry, and D. K. Schwartz, *J. Am. Chem. Soc.* **136**, 1327 (2014).
- 52 O. V. Bychuk and B. O'Shaughnessy, *J. Chem. Phys.* **101**, 772 (1994).
- 53 D. Wang and D. K. Schwartz, *J. Phys. Chem. C* **124**, 19880 (2020).
- 54 C. Ö. Diñç, G. Kibarar, and A. Güner, *J. Appl. Polym. Sci.* **117**, 1100 (2010).
- 55 T. Kato, K. Nakamura, M. Kawaguchi, and A. Takahashi, *Polym. J.* **13**, 1037 (1981).
- 56 C. White, K. T. Tan, D. Hunston, K. Steffens, D. L. Stanley, S. K. Satija, B. Akgun, and B. D. Vogt, *Soft Matter* **11**, 3994 (2015).
- 57 Y. Zhang and Z. Fakhraei, *Proc. Natl. Acad. Sci. U. S. A.* **114**, 4915 (2017).
- 58 W. M. Stanley and T. F. Anderson, *J. Biol. Chem.* **139**, 325 (1941).
- 59 T. B. Karim and G. B. McKenna, *Polymer* **54**, 5928 (2013).
- 60 M. Mears *et al.*, The University of Sheffield. Dataset <https://doi.org/10.15131/shef.data.14390495> (2021).